MCB
Journals.ASM.org

Cytoplasmic Poly(A) Binding Protein C4 Serves a Critical Role in Erythroid Differentiation

Hemant K. Kini,[a] Jian Kong,[a] Stephen A. Liebhaber[a,b]

Departments of Genetics[a] and Medicine,[b] Perelman School of Medicine, University of Pennsylvania, Philadelphia, Pennsylvania, USA

The expression of an mRNA is strongly impacted by its 3′ poly(A) tail and associated poly(A)-binding proteins (PABPs). Vertebrates encode six PABP isoforms that vary in abundance, distribution, developmental control, and subcellular localization. Here we demonstrate that the minor PABP isoform PABPC4 is expressed in erythroid cells and impacts the steady-state expression of a subset of erythroid mRNAs. Motif analyses reveal a high-value AU-rich motif in the 3′ untranslated regions (UTRs) of PABPC4-impacted mRNAs. This motif enhances the association of PABPC4 with mRNAs containing critically shortened poly(A) tails. This association may serve to protect a subset of mRNAs from accelerated decay. Finally, we demonstrate that selective depletion of PABPC4 in an erythroblast cell line inhibits terminal erythroid maturation with corresponding alterations in the erythroid gene expression. These observations lead us to conclude that PABPC4 plays an essential role in posttranscriptional control of a major developmental pathway.

Poly(A) tails are added posttranscriptionally to the 3′ termini of all nonhistone PolII transcripts (1, 2). These poly(A) tails are bound by a family of six distinct poly(A)-binding proteins (PABPs). These PABP isoforms demonstrate diversity in their abundance, cellular localization, developmental control, and tissue specificity. All six isoforms share a high affinity and specificity for poly(A) tracts. In vertebrate species, a single nuclear poly(A)-binding protein (PABPN1) participates in 3′ processing of PolII transcripts (3). The remaining five PABP isoforms are cytoplasmic. The major cytoplasmic PABP isoform in adult somatic tissues is PABPC1. Four minor cytoplasmic isoforms have also been described. An embryonic poly(A)-binding protein (ePAB), expressed in oocytes and early embryos (4, 5), regulates the stability and translational activity of maternal mRNAs (6) and retains selective expression in adult ovaries and testes. The remaining three minor PABP isoforms are a testis-specific PABP (tPABP, or PABPC2 in the mouse), a PABP identified as an inducible protein in stimulated T cells (iPABP or PABPC4), and X-linked PABP (PABPC5) (7–9). With the possible exception of the ePAB, there exists minimal information on specific roles and activities of any of the minor PABP isoforms.

Current understanding of PABP functions is based primarily on studies of PABPN1 (nuclear functions) and PABPC1 (cytoplasmic functions). Multiple studies support a critical role of PABPC1 in the enhancement of mRNA expression via simultaneous binding to the 3′ poly(A) tail and the 5′ cap complex (10, 11). The ensuing closed-loop structure is thought to facilitate mRNA translation via ribosome recycling while also protecting the transcript from exonucleolytic decay (12–14). In contrast, tPABP (PABPC2) appears to repress translation of mRNAs during spermatogenesis (15).

The least studied PABP isoform is PABPC4. Although this minor isoform was initially identified as a protein that is induced following human T-cell activation, its role in this process has not been further explored (8). A recent study demonstrated that selective depletion of PABPC4 in *Xenopus laevis* embryos interferes with tadpole development (16). Importantly, this developmental defect could not be compensated for by either PABPC1 or ePAB. Whether PABPC4 plays a nonredundant and critical role in mammalian somatic-cell development and function remains unexplored.

Posttranscriptional controls are most apparent in settings where transcriptional controls are no longer paramount. Terminal differentiation of specific somatic and germ cells is of particular importance in this regard. The terminal differentiation of red cells is perhaps the most extreme example, as it involves a global silencing of transcription midway through the differentiation process (17). Thus, the final phases of red-cell formation are entirely dependent on controls over mRNA stability and translational activity (18, 19).

Mouse erythroleukemia (MEL) cells (20) are a commonly used model of erythroid differentiation. These cells correspond to the proerythroblast stage of red-cell differentiation and can be induced to terminally differentiate by a variety of chemical agents, most commonly dimethyl sulfoxide (DMSO). As MEL cells progress through the differentiation process, they undergo a decrease in cell size and marked nuclear compaction (21, 22). The terminal events in this differentiation process occur in a transcriptionally silent setting, rendering them entirely dependent on posttranscriptional controls. Most prominent among these controls is the high-level stabilization of mRNAs critical to the final phases of red-cell formation and subsequent function. In prior studies, we described the role of the poly(C)-binding protein, αCP, in stabilization of *hα-globin* mRNA (23–26). The poly(A) tail of the *hα-globin* mRNA undergoes progressive shortening during erythroid differentiation *in vivo*, and this shortening is dependent on stability determinants within the 3′ untranslated region (UTR) (27). Here we focused on a second protein, PABPC4, which asso-

Received 19 December 2013 Returned for modification 8 January 2014
Accepted 16 January 2014
Published ahead of print 27 January 2014
Address correspondence to Stephen A. Liebhaber, liebhabe@mail.med.upenn.edu.

doi:10.1128/MCB.01683-13

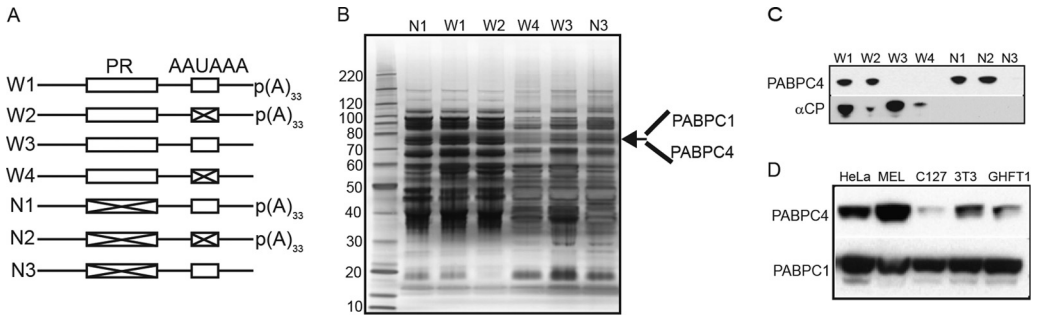

FIG 1 The PABP isoform PABPC4 associates with the *hα-globin* mRNA 3′ UTR and is highly expressed in mouse erythroleukemia cells. (A) *hα-globin* 3′ UTRs used in the affinity pulldowns. Three major determinants of *hα-globin* mRNA expression are shown in the diagram; the C-rich αCP binding site (protected region [PR]), the AAUAAA signal (cleavage and polyadenylation signal), and a poly(A_{33}) tail. These determinants were mutated or deleted in various combinations, and the impact of each mutation on protein interactions was determined. (B) Display of proteins bound to the RNA affinity matrix. The silver-stained gel image reveals proteins from MEL cell that were bound to each of the *hα-globin* mRNAs shown in panel A. The arrow indicates protein bands that were identified by mass spectrometry as comigrating PABPC1 and PABPC4. (C) Western analysis of affinity pulldowns with *hα-globin* 3′ UTR elements with antibodies against PABPC4 and αCP2. (D) Western analysis profiling of PABPC4 and PABPC1 proteins in cell culture lines. PABPC4 was exposed 15 times longer than PABPC1 to compensate for its overall lower expression. The enrichment for PABPC4 relative to the predominant PABPC1 isoform in the MEL cells compared to each of the other cell lines is evident.

ciates with the *hα-globin* mRNA 3′ UTR, impacts poly(A) functions, and controls mRNA expression. Our data lead us to conclude that PABPC4 plays a critical and nonredundant role in a major developmental pathway.

MATERIALS AND METHODS

Cell culture and transfection. MEL and Plat-E cells (28) were grown under standard conditions in minimal essential medium (MEM) and Dulbecco's modified Eagle medium (DMEM), respectively, supplemented with 10% (vol/vol) fetal bovine serum (FBS) and 1× antibiotic-antimycotic (Invitrogen). MEL cells in suspension culture at the log phase of growth at a density of 2×10^5/ml were supplemented with 2% DMSO (Sigma) to induce differentiation, and cells were collected at various time points for biochemical assays.

Affinity enrichment of RNA-protein complexes. The cDNAs encoding the 3′ UTR of the wild-type (WT) *hα-globin* mRNA with a poly(A) tail (WT-pA-A33; W1), with a poly(A) tail but lacking a functional nuclear poly(A) signal (WT-pA-A33; W2), lacking a poly(A) tail (WT-pA; W3), and lacking both the poly(A) tail and functional poly(A) signal (WT-pA−; W4) were each inserted into pSP64 vector with a 5′-terminal T7 promoter (Fig. 1A). A corresponding set of cDNAs, N1, N2, and N3 (Fig. 1A), with disabled αCP binding sequences were cloned in parallel. Each 3′ UTR RNA was transcribed *in vitro* from the T7 promoter (Megashort Script T7 *in vitro* transcription kit; Life Technologies), oxidized, and covalently linked to adipic acid dihydrazide-agarose beads (29, 30). The beads were incubated with S16 MEL cell cytoplasmic extract, and the bound proteins were eluted and resolved on SDS-PAGE. For the IRF7 3′ UTR variants, cDNAs encoding the WT or mutant IRF7 3′ UTR-containing 5′ terminal T7 promoter sequences were chemically synthesized as single-stranded oligonucleotides (Invitrogen). The strands were annealed to generate double-stranded DNA (dsDNA) templates for *in vitro* transcription, and the affinity pulldowns were performed as described above.

Generating stable cell lines. (i) Virus production. Plate-E cells were plated at a density of 50,000/ml in 60-mm plates 1 day prior to transfection. Short hairpin RNAs (shRNAs) targeting PABPC4 mRNA and the control scrambled shRNA were purchased from Origene (Rockville, MD). A 6-μg portion of each shRNA in the p-GFP-V-RS vector was transfected using Mirus TransIT-293 reagent per the manufacturer's recommendation. At 24 h posttransfection, the cells were transferred to fresh medium, and after an additional 24 h of incubation, the cell supernatant containing shed virus was harvested.

(ii) Cell transfection. MEL cells were plated at 100,000/ml in 6-well plates. One day after plating, these cells were infected with 500 μl of shRNA encoding viral supernatants supplemented with 500 μl of medium and 8 μg of Polybrene (Sigma). Following 24 h of incubation, the cells were placed under selection for 6 days in medium containing 1.2 μg of puromycin/ml and then maintained in medium with 0.2 μg of puromycin/ml. PABPC4 depletion was assayed by Western blotting and quantitative reverse transcription-PCR (qRT-PCR). For Western analysis, the cells were lysed in radioimmunoprecipitation assay (RIPA) buffer, and the following primary and secondary antibodies were used: rabbit anti-PABPC4 (Bethyl), rabbit anti-PABPC1 (Bethyl), rabbit antiactin (Bethyl), and anti-rabbit IgG–horseradish peroxidase (HRP) conjugate (Cell Signaling Technology). For RNA analysis, total cellular RNA was harvested (Qiagen miRNeasy kit) from each of three independent cell pools expressing either a scrambled shRNA (sh-Scr) or an shRNA targeting PABPC4 (sh-C4-58, sh-C4-60, or sh-C4-8). cDNA synthesis was primed with random hexamers and oligo(dT). qPCR was performed on an ABI fast 7500 platform. Primer and shRNA sequences are provided in Table 1.

Microarray analysis. RNAs converted to biotinylated cRNAs were hybridized to an Affymetrix mouse gene 1.0 ST oligonucleotide array containing probes corresponding to approximately 28,000 genes. Each of the array hybridizations was performed in triplicate. cRNA syntheses and array hybridizations were performed by the University of Pennsylvania microarray facility. CEL files containing the array hybridization intensity data were imported and analyzed with the Partek genomics suite. Data were normalized with the robust multichip average algorithm (31).

Cross-linking, immunoprecipitation, and microarray analyses. MEL cells in a minimal volume of phosphate-buffered saline (PBS) were UV cross-linked at 400 mJ/cm^2 in a Stratalinker and lysed in detergent buffer (50 mM HEPES, 150 mM NaCl, 10 mM $MgCl_2$, 0.6% Empigen, 0.1 mM dithiothreitol [DTT]) prior to immunoprecipitation. Protein G beads were washed four times with diethyl pyrocarbonate (DEPC) water, twice with PBS, and finally once with buffer X (50 mM HEPES, 200 mM NaCl, 10 mM $MgCl_2$, 0.2% Empigen). Antibody or rabbit IgG (2 μg) was preincubated with 250 μl of cell extracts and 150 μl of lysis buffer for 3 h at 4°C. Protein G-Sepharose beads were added to these reactions and incubated for 45 min. Beads then underwent four successive washes in buffer W1 (50 mM HEPES, 200 mM NaCl, 10 mM $MgCl_2$, 1.2% Empigen) and two additional washes with buffer W2 (50 mM HEPES, 200 mM NaCl, 10 mM $MgCl_2$, 0.2% Empigen). Each wash was for 10 min at 4°C. The washed IP material was then digested in 15 μl of proteinase K in a 200-μl reaction volume at 37°C for 1 h (50 mM Tris [pH 7.5], 150 mM NaCl, 1% SDS, 0.5 mM EDTA). RNA was extracted from the digest with a Qiagen miRNeasy kit.

TABLE 1 Primer and shRNA sequences

Primer or shRNA	Sequence(s)[a]
Primers	
β-Actin	GACAGGATGCAGAAGGAGATTACTG/CTCAGGAGGAGC AATGATCTTGAT
Btg2	GAGCAGAGACTCAAGGTTTTCAGTAG/GCGATAGCCAG AACCTTTGG
Cd44	GCCGTCTGCATCGCGGTCAATA/CCGTCCCATTGCCAC CGTTGAT
c-Kit	GCCACGTCTCAGCCATCTG/GTCGCCAGCTTCAACTAT TAACT
c-Myb	TGACTTTCGACACATGGCTCCTCA/AATGCACTTGGTG CTGCTCTCAAC
c-Myc	CACCACCAGCAGCGACTCTGAA/ATGAGCCCGACTCCG ACCTCTT
GAPDH	TGTCAAGCTCATTTCCTGGTATGA/TCTTACTCCTTGGA GGCCATGT
GATA1	GCCCAAGAAGCGAATGATTG/GTGGTCGTTTGACAGTT AGTGCAT
GATA2	CACCCCTAAGCAGAGAAGCAA/TGGCACCACAGTTGA CACACT
Gypa	CCATCATTGTCAGGATCAGATTCTC/CATTGTTGCTGA ATGCTGATTTG
α-Globin	CCTGGAAAGGATGTTTGCTAGCT/GCCGTGGCTTACAT CAAAGTG
β-Globin	GCACCTGACTGATGCTGAGAA/TTCATCGGCGTTCACC TTTCC
PABPC1	GCGCAGAAAGCTGTGGATG/TTTGCGCTTAAGTTCCGTC
PABPC4	ATCTGGCTCCAACTGGTAATGC/GCTGTCAGTCAGCCC TTGCT
Stat5a	GTTTGAGTCTCAGTTCAGCGT/CATGGACGATAACGAC CACAG
shRNAs	
PAT	GCGAGCTCCGCGGCCGCGTTTTTTTTTTTT
PAT-TVN	GCGAGCTCCGCGGCCGCGTTTTTTTTTTTTVN
Hba-a1 PAT	TGCTGACCTCCAAGTACCGT
Samd9l-PAT	TCCATACCACAGAGCTTGGC
Hbb-b1-PAT	GCCCCTTTTCTGCTATTGTCT
GAPDH-PAT	ACTGAGCAAGAGAGGCCCTA
β-Actin-PAT	TGAGGTGTTGAGGCAGCCAG
sh-Scr	GCACTACCAGAGCTAACTCAGATAGTACT
sh-C4-60	CTGTCACCGAGATGAATGGACGCATTGTG
sh-C4-58	AACACGAGGATGCCAATAAGGCTGTGGAA
sh-C4-68	CTTCACCAATGTTTATATCA

[a] Primer sequences are given as forward/reverse.

Flow cytometry. Cells were stained with c-Kit antibody (BD) and were analyzed on a FACSCanto II flow cytometer (BD Bioscience) using FlowJo software (Tree Star Inc.).

Extension poly(A) test (ePAT). The PAT and TVN poly(A) tail assays were performed as described previously (32). One microgram of total RNA and 1 μl (100 mM) of PAT anchor primer were used in the polymerization reaction (Klenow polymerase; New England BioLabs) and subsequent cDNA synthesis with Superscript III reverse transcriptase (Life Technologies). The cDNA reaction mixture was diluted (1:6 ratio), and 5 μl of this was used in a 20-μl PCR mixture with gene-specific primers. PCR products were resolved on 2% high-resolution Tris-borate-EDTA—agarose gel (Ultrapure 1000; Life Technologies). Gels were prestained with SYBR Safe (Life Technologies), and a TrackIt 100-bp DNA ladder (Life Technologies) was used as a size marker. Primer sequences are provided in Table 1.

RESULTS

PABPC4 binds to the *hα-globin* mRNA 3′ UTR. We previously identified an RNA surveillance pathway that targets the decay of *hα-globin* mRNAs containing antitermination mutations (33). This pathway, triggered by extension of an antiterminated ribosome into the 3′ UTR, was termed ribosome extension-mediated decay (REMD) (33). We observed that the antiterminated ribosome displaces the αCP stability complex from the 3′ UTR (26, 33). While the impact of αCP displacement could be clearly detected by a discrete drop in the *hα-globin* mRNA half-life, the antiterminated ribosome triggered a second drop-off in stability as it extended further toward the mRNA 3′ terminus. To characterize this second destabilization event and identify the corresponding 3′-terminal stability determinant, we performed affinity pulldowns with the *hα-globin* 3′ UTR and a set of informative derivatives (Fig. 1A). Proteins bound to each of the 3′ UTR fragments were separated by gel electrophoresis and identified by mass spectrometry. Prominent among these proteins was PABPC4 (Fig. 1B and C). PABPC4 was of particular interest due to its relative enrichment in the erythroleukemia cell line MEL (Fig. 1D) and due to the well-known impact of PABPs on poly(A) tail metabolism and mRNA expression.

Selective depletion of PABPC4 in MEL cells. The contribution of PABPC4 to the steady-state erythroid transcriptome was explored via shRNA-mediated depletion of PABPC4 in the mouse erythroleukemia (MEL) cell line. MEL cells in maintenance phase were infected with a set of shRNA-encoding retroviruses targeting PABPC4 mRNA. Three distinct shRNAs were used in these studies (sh-C4-60, sh-C4-58, and sh-C4-68). Each shRNA targeted a different site on the PABPC4 mRNA in order to control for off-target effects. Two additional controls were established: virus containing a scrambled sequence shRNA (sh-Scr) and a population of untransfected MEL cells. Each of the PABPC4-targeting shRNAs resulted in a 70% or greater depletion of PABPC4 mRNA and protein (Fig. 2A and B). There was no apparent impact of these PABPC4-targeting shRNAs on expression of the major PABP isoform, PABPC1. Thus, all three distinct shRNAs were highly effective and specific in establishing MEL cell pools depleted of PABPC4.

PABPC4 depletion in MEL cells has a minimal impact on total PABP content. PABPC1 is the predominant PABP isoform in the cytoplasm of most eukaryotic cells, existing in gross excess over PABPC4 (34). Quantitative assessment of this relationship in MEL cells (see Materials and Methods) revealed that PABPC1 mRNA is present at 11-fold-higher levels than PABPC4 mRNA (Fig. 2C). These data, which are consistent with the Western analysis (Fig. 1D), lead us to conclude that the PABPC4 shRNAs, while effective in clearing PABPC4 from the MEL cells (Fig. 2A and B), have a minimal impact on the overall levels of PABP activity. Thus, any general functions attributable to PABP activity in these cells should be preserved in the PABPC4-depleted MEL cells, and any impact of PABPC4 depletion on the cell should reflect one or more functions that are specific to PABPC4 and not shared with PABPC1.

PABPC4 depletion impacts steady-state levels of a subset of mRNAs. Total RNA extracted from a PABPC4-depleted MEL cell pool (sh-C4-60) and from a parallel control pool (sh-Scr) were converted to cRNA and subjected to microarray analysis (Affymetrix mouse gene 1.0 ST). Each analysis was performed in triplicate beginning with RNA from six separate pools expressing either sh-C4-60 or sh-Scr. The fold change (FC) in expression represents the average difference in expression between the sh-Scr and sh-C4-60 samples. This FC value was computed for the each gene on the array along with the corresponding significance *Q* value (see Materials and Methods).

The microarray analyses revealed 58 mRNAs with a 2-fold or greater change in expression in the PABPC4 depletion (*Q* values $<$ 0.05) (data not shown). To validate the microarray results, we determined the alteration in the expression of 23 impacted and 4 nonimpacted mRNAs by qRT-PCR (data not shown). Of these,

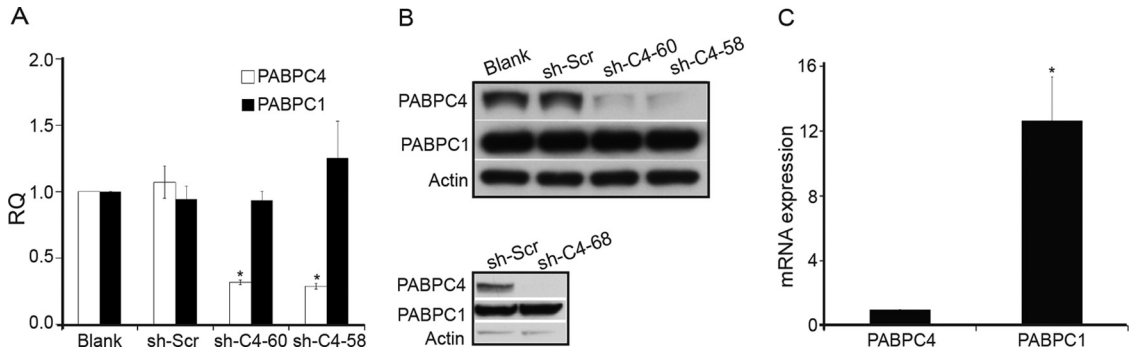

FIG 2 Selective depletion of PABPC4 from MEL cells is isoform specific and has minimal impact on overall levels of PABP activity. (A) Assessment of PABPC4 mRNA depletion in cells transformed with shRNA-expressing retrovirus. mRNA levels were quantified by qRT-PCR. All experiments were done in biologic triplicates. Error bars represent one standard deviation ($n = 3$). Asterisks denote P values (one-tailed t test) of less than 0.05 for the PABPC4 knockdown pools compared to the untransfected MEL cell pools (blank). (B) Targeted depletion of PABPC4 is isoform specific. The Western analysis monitors protein levels of PABPC4, PABPC1, and a loading control (actin). sh-Scr contains a scrambled sequence, and sh-C4-60, sh-C4-58, and sh-C4-68 target different regions of PABPC4 mRNA. (C) Expression of PABPC1 mRNA in MEL cells exceeds PABPC4 mRNA more than 11-fold. qRT-PCR studies were carried out with primer sets of equivalent efficiencies. The asterisk denotes a P value (one-tailed t test) of less than 0.05 for PABPC1 expression compared to PABPC4. β-Actin and GAPDH were both used as internal normalization controls for all qRT-PCRs.

the altered expression could be validated in all but two mRNAs (BMP6 and Abcb1a) in the sh-58 pool. These two mRNAs were eliminated from subsequent analysis. Among the mRNAs demonstrated to respond to the PABPC4 depletion were those involved in pathways critical to cell growth (Acer2; cell proliferation and survival [35]), metabolism (Acadl; type 1 diabetes [36]), transformation (Antxr1; tumorigenesis [37]), and erythroid differentiation (α-globin; erythropoiesis [38]). These studies indicated that PABPC4 exerts control over the steady-state expression of a subset of mRNAs and that this control is nonredundant with the far more abundant PABPC1.

Identification of mRNAs enriched in PABPC4 complexes. The identified alterations in the MEL cell transcriptome in response to PABPC4 depletion could reflect primary interactions of PABPC4 with target mRNAs, or they could reflect secondary effects. To distinguish these two possibilities, we proceeded to identify mRNAs physically associated with PABPC4.

MEL cells in maintenance culture were exposed to UV light to cross-link mRNP complexes. The PABPC4-associated complexes were immunoprecipitated with either PABPC4 antisera or preimmune serum. The effectiveness of the PABPC4 IP was confirmed by Western analysis (Fig. 3, inset), and mRNAs isolated from proteinase-treated IP pellets were assessed for enrichment by microarray analysis (Affymetrix mouse gene 1.0 ST chip). Each study was done in triplicate beginning with RNA extracted from six separate PABPC4-IP and control IP reactions. The average difference in signal intensities in the anti-PABPC4 pellet versus the preimmune IgG pellet was used to calculate a relative fold enrichment (FE) value for each mRNA (see Materials and Methods). A set of 140 mRNAs whose steady-state levels were unaffected by PABPC4 depletion was used to calculate a background enrichment value. The average FE value in this control group was 4.5. We set the fold enrichment criterion for the direct binding targets as 4.95 (10% over the control group enrichment of 4.5). Notably, 31 of the 58 mRNAs (54.4%) with a >2-fold change in steady-state expression subsequent to PABPC4 depletion were enriched above the 4.95-fold enrichment cutoff in the PABPC4 IP. This compares with a far lower frequency of enrichment in PABPC4 complexes for mRNAs that were not altered in the steady state (29 out of 140; 20.7%), suggesting a strong correlation between association of PABPC4 with a transcript and its level of expression. The set of 13 mRNAs whose steady-state levels were increased 2-fold or more in the PABPC4-depleted cells had a mean FE value of 8.4, and the set of 18 mRNAs that were decreased 2-fold or more had a mean FE value of 6.4. *In vivo* association of two of these functional targets with PABPC4, α-globin, and IRF7 mRNAs was confirmed by RNA-IP followed by qRT-PCR analysis (data not shown). These data lead us to conclude that a substantial number of mRNAs impacted in steady-state expression by PABPC4 are associated with PABPC4 *in vivo* (Fig. 3 and Table 2).

Depletion of PABPC4 in MEL cells results in a selective loss of target mRNAs with short poly(A) tails. To address the mech-

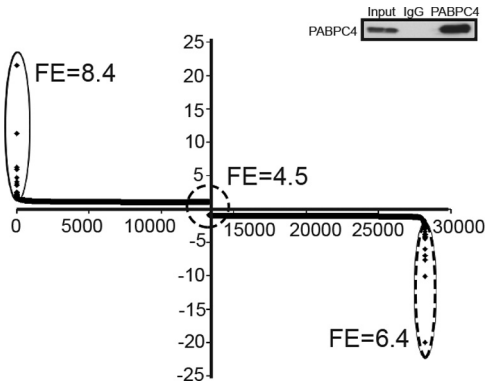

FIG 3 The subsets of mRNAs impacted by PABPC4 depletion demonstrate mean enrichment in immunoprecipitated PABPC4 mRNP complexes. The fold change (positive or negative) in steady-state mRNA levels subsequent to PABPC4 depletion in MEL cells (Affymetrix mouse gene 1.0 ST) is displayed on the y axis. The x axis is the numerical representation of the genes on the array. The ovals encompass sets of mRNAs that were enhanced more than 2-fold (solid oval, 13 mRNAs), unaffected (dashed oval, 140 genes), or downregulated more than 2-fold (broken oval, 18 genes). The mean fold enrichments (FE) for each set of mRNAs in the immunoprecipitated PABPC4 complexes are indicated. The fold enrichment calculation is described in Materials and Methods. (Inset) Western blot analysis confirmed the enrichment of PABPC4 protein in the PABPC4 IP relative to the IgG control.

TABLE 2 mRNAs that constitute direct and functional targets of PABPC4

Gene class and mRNA[a]	FC	FE
Upregulated by PABPC4 depletion		
Acadl	6.0	9.4
Acer2	21.5	10.4
Aim2	3.8	5.8
Bcs1l	2.0	11.7
Ccnyl1	2.2	13.0
Cd38	2.2	6.6
Cdc42ep2	2.3	6.8
Ceacam2	2.5	5.5
Cpa3	2.5	6.2
Cytip	2.1	5.6
Egln3	2.2	15.8
Slc18a2	2.4	5.3
Tmem40	3.6	6.7
Downregulated by PABPC4 depletion		
Cmpk2	−2.0	5.5
Csprs	−2.4	5.6
α-Globin	−2.2	5.3
α-Globin 2	−2.2	5.8
H2-T24	−2.2	5.3
Ifih1	−2.0	5.1
Ifit1	−2.1	6.0
Il12rb2	−2.1	5.0
Irf7	−2.3	12.0
Irgm1	−3.0	6.5
Oas2	−2.4	5.3
Oasl2	−3.4	5.7
Rgs2	−2.0	7.0
Rtp4	−6.0	8.6
Samd9l	−2.0	10.1
Sp100	−3.8	5.0
Tgtp1	−3.0	5.5
Tmem206	−7.0	5.0

[a] The mRNAs listed satisfy two criteria: fold change (FC) in expression (up or down) of ≥2-fold in steady state by PABPC4 depletion and fold enrichment (FE) of more than 4.95 (10% over the 4.5 enrichment of the control group) in the immunoprecipitated PABPC4 RNP complexes.

anism by which PABPC4 impacts selected mRNAs, we determined its impact on poly(A) tail size distributions (by ePAT) (32). The poly(A) tail distributions of two housekeeping mRNAs whose levels were unaffected by the PABPC4 depletion were unchanged subsequent to PABPC4 depletion (glyceraldehyde-3-phosphate dehydrogenase [GAPDH] and β-actin) (Fig. 4E to H). We next tested two mRNAs, α-*globin* and *Samd9l*, whose steady-state levels were both impacted by PABPC4 depletion and were enriched in the PABPC4 complexes (Table 2). For both of these mRNAs, the PABPC4 depletion resulted in a selective loss of mRNAs with short poly(A) tails (<30 A's), while the populations with longer poly(A) tails were unaffected (Fig. 4A to D). To determine if this effect of PABPC4 depletion on the short-poly(A)-tailed mRNAs relates to alterations in mRNA steady-state levels, we performed ePAT analysis on β-*globin* mRNA. β-*globin* mRNA is enriched in PABPC4 mRNP complexes (Table 3), but its expression is not affected to the same level as that of α-*globin* mRNA or the other direct functional targets of PABPC4 (functional targets are listed in Table 2). ePAT analysis of β-*globin* mRNA revealed that the ratio of long to short poly(A) tails is unaffected by PABPC4 depletion (Fig. 4I and J). These data are consistent with a model in which PABPC4 can bind mRNAs with critically shortened poly(A) tails and protect the corresponding mRNA molecule from accelerated decay.

PABPC4-targeted mRNAs are marked by a 3′ UTR AU-rich motif. The basis for the selective targeting of an mRNA subset by PABPC4 was next addressed. A motif search (MEME) was carried out on the 3′ UTR sequences corresponding to the 31 mRNAs identified as direct binding targets of PABPC4 (Table 2) (39). To enhance the value of the study, we compared these mRNAs to a negative pool of 31 mRNAs that were not impacted by PABPC4 depletion and not enriched in PABPC4 complexes (FE < 2.0). We assumed in this analysis that these negative-control mRNAs did not possess a putative PABPC4 binding motif. Using these negative mRNAs as the background control for the motif search, we performed discriminative motif discovery in MEME. This analysis yielded several motifs. The highest rank-valued motif (Fig. 5A) was a 12-nucleotide (nt) AU-rich sequence. Remarkably, this motif was present in the 3′ UTRs of all 31 of the PABPC4 functional targets. The identification of this motif as underlying the specificity of PABPC4 actions on mRNA expression is consistent with a prior report that that PABPC4 binds to AU-rich sequences through its RNA-binding domains 3 and 4 (40).

The influence of this AU-rich motif on PABPC4 binding to a target mRNA was next explored. The 3′ UTR of the IRF7 mRNA was chosen for detailed analysis based on its short size (42 nt) and its high level of enrichment in PABPC4 RNP complexes (FE = 12.0) (Fig. 5B). An *in vitro*-transcribed IRF7 3′ UTR was cross-linked to beads, and this affinity matrix was used to identify interacting proteins from MEL cell extracts. We first determined the minimal length of the poly(A) tail on the IRF7 3′ UTR that would bind PABP under our affinity conditions (data not shown). This A_{12} length agrees well with the minimum PABP binding site identified in budding yeast (41). The polyadenylation signal, AAUAAA, constitutes a segment of the AU-rich motif in this mRNA. A mutant IRF7 3′ UTR RNA containing a minimal poly(A_{12}) tail and a poly(A) signal converted to a random sequence was generated (Fig. 5B, sequence M1). This mutant sequence had a significantly compromised PABPC4 binding activity, whereas the parallel assessment of PABPC1 binding showed that it was unaffected (Fig. 5C). These data reveal that the AU-rich binding motif can enhance the binding of PABPC4 to an mRNA with a critically shortened poly(A) tail.

Annotation analysis of PABPC4 functional targets. To explore the role(s) of PABPC4 in cell function, we performed annotation clustering. Each of the 31 mRNAs included in this analysis had to satisfy two distinct criteria in order to be characterized as a direct functional target: alteration in steady-state expression by >2-fold (up or down) in cells depleted of PABPC4 and enrichment above control levels in the immunoprecipitated PABPC4 RNP complexes (Table 2). A total of 4,850 curated gene sets were mined utilizing gene set enrichment analysis (GSEA) (42, 43) with a filter set for a false discovery rate (FDR) *Q* value of <0.25. The gene sets identified in this analysis overlapped four pathways (in rank order); hematopoietic stem cell differentiation ($P = 0.0005$) (44), oxidative phosphorylation ($P = 0.043$) (42), nasopharyngeal carcinoma ($P = 0.025$), and Ewing sarcoma ($P = 0.016$) (45, 46). Importantly, this group of 31 RNAs contained two globin RNAs, Hba-a1 and Hba-a2. An additional 11 mRNAs that satisfied one of the two criteria used to identify the functional targets of PABPC4 were prominent in the erythropoiesis pathway (Table 3). These

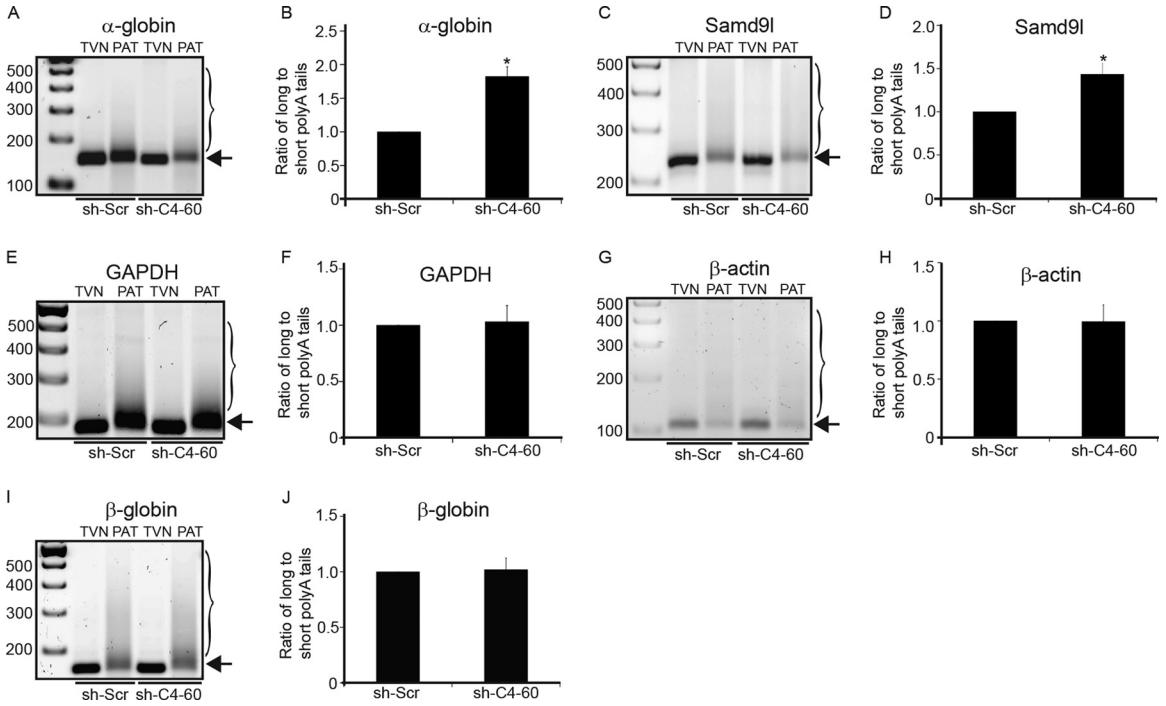

FIG 4 PABPC4 depletion alters the ratio of long to short poly(A) tails of targeted mRNAs. (A, C, E, G, and I) Poly(A) tail analyses (by ePAT; see Materials and Methods) of α-*globin*, *Samd9l*, *GAPDH*, β-*actin*, and β-*globin* mRNAs. The arrows and brackets identify the positions of the short and long poly(A) tails, respectively. (B, D, F, H, and J) Densitometric quantifications of the poly(A)-tail indexes (*y* axis). This index corresponds to a ratio of long to short poly(A) tails for each indicated mRNA in either the control (sh-Scr) or the PABPC4-depleted (sh-C4-60) MEL cells. The data in each histogram are averages from multiple studies ($n \geq 3$). Asterisks denote *P* values (one-tailed *t* test) of less than 0.05 for the PABPC4-depleted pool (sh-C4-60) compared to the control pool (sh-Scr). PAT lanes show the poly(A) tail distribution of mRNAs, and the TVN lanes represent the amplicon with an invariant 12-nt poly(A) tail.

data suggested that PABPC4 might play a role in erythropoiesis and/or terminal erythroid differentiation.

Erythroid differentiation is blunted in PABPC4-depleted MEL cells. To assess the importance of PABPC4 in erythroid differentiation, we first confirmed the expression of this isoform in MEL cells during the differentiation process (Fig. 6) and then monitored the impact of PABPC4 depletion on this process. Visual comparison of the PABPC4-depleted MEL cell pool to a parallel MEL cell pool expressing the control sh-Scr revealed a delay

TABLE 3 mRNAs related to terminal erythroid differentiation

mRNA[a]	FC	FE	*Q* value
α-Globin	−2.2	5.3	0
α-Globin 2	−2.2	5.8	0
Alas2	−1.6	8.4	3.99
β-Globin	−1.6	5.8	2.04
Bnip3	1.6	8.4	0
Casp7	1.2	5.2	2.04
Casp8	1.1	7.3	3.99
Gata2	1.1	5.6	3.99
Gypa	−1.5	8.8	0
Hif1a	1.5	5.4	0
Il12rb2	−2.1	5.0	0
Spna1	−4.3	4.1	0
Tcfcp2	1.2	6.1	0.38

[a] mRNAs whose fold change (FC) in steady-state expression levels is ≥2 following PABPC4 depletion and/or whose fold enrichment (FE) scores are more than 4.95 (10% over the 4.5 enrichment of the control group) in the immunoprecipitated PABPC4 RNP complexes.

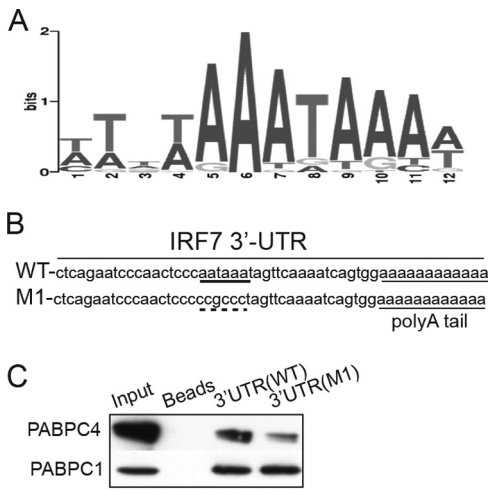

FIG 5 PABPC4 binding to an RNA with critically shortened poly(A) tail is enhanced by an adjacent AU-rich determinant. (A) MEME analysis of 3′ UTR sequences of 31 direct functional targets of PABPC4 reveals a high-value AU-rich motif (E-value, 2.3e−037). Other binding motifs were also predicted but with significantly lower E values than the motif shown (data not shown). (B) Impact of the AU-rich determinant on PABPC4 binding to a PABPC4-targeted mRNA (IRF7). The AAUAAA signal in the WT was replaced with a set of CG substitutions (M1). Both the WT and the M1 RNAs contain a minimal (A_{12}) tail. (C) Western blot analysis of MEL proteins enriched by affinity pull-downs with the indicated 3′ UTR elements (WT or M1). The data reveal that PABPC4 binding to the RNA with a minimal poly(A) tail is enhanced by the adjacent AU-rich motif, while binding by PABPC1 is unaffected by the presence of this determinant.

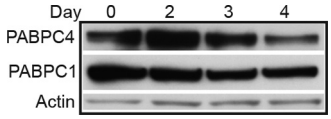

FIG 6 Survey of PABPC1 and C4 expression in MEL cells during terminal erythroid maturation. Western analysis of PABP expression was carried out at days 0, 2, 3, and 4 following DMSO induction. Actin is included in the analysis as a loading control.

in hemoglobin accumulation (Fig. 7A). This difference was confirmed with a quantitative assay of hemoglobin content (Drabkin's assay) (Fig. 7B).

To further assess the impact of PABPC4 on MEL cell differentiation at the level of gene expression, we assayed five genes that are normally induced during terminal differentiation, encoding the following proteins: α- and β-globin (Hba-a1 and Hbb-b1); glycophorin A (Gypa); solute carrier family 4, anion exchanger, member 1 (Slc4a1); and B-cell translocation gene 2 (Btg2) (Fig. 8A to E). mRNA steady-state levels were calculated relative to the uninduced sh-Scr pool (whose level was defined as 1.0). Remarkably, the expression of each of these genes, normally robustly induced by DMSO during terminal differentiation, was significantly repressed by PABPC4 depletion.

We next assessed the expression of a set of mRNAs encoding regulatory proteins that are normally expressed at high levels in the early erythroid stage and undergo repression during terminal differentiation. These genes encode c-myc, c-myb, CD44, Stat5a, and c-Kit (Fig. 8F to J). There was no noticeable impact of the PABPC4 depletion on the mRNA expression of the first four of these genes at 72 h of differentiation. In contrast, c-Kit mRNA was abnormally elevated in the uninduced PABPC4-depleted cells and remained abnormally elevated upon DMSO induction. Repression of c-Kit expression is considered to be a prerequisite for the erythroblast to enter the terminal phases of erythroid differentiation (47). The abnormally elevated levels of c-Kit expression in the DMSO-induced PABPC4-depleted cells were confirmed by FACS analyses (data not shown). Thus, the blunting of globin gene induction and the blockade of red-cell differentiation are consistent with the sustained expression of c-Kit in the PABPC4-depleted MEL cells (Fig. 8J).

DISCUSSION

A fundamental question addressed in this report is whether the functions of the minor PABP isoform PABPC4 are distinct from those of the major isoform, PABPC1, when assessed in a mammalian cellular context. While both PABP isoforms share a high affinity and specificity for binding to poly(A) homopolymer tracts, evidence suggests that their binding specificities and biologic functions may differ. This possibility is supported by the structural divergence in the RNA recognition motif (RRM) 3-4 domains of these two isoforms (40) and by the demonstration of a nonredundant role for PABPC4 in a *Xenopus* tadpole development (16). To address this question in a mammalian developmental context, we selectively depleted PABPC4 from a well-defined and intensively studied mouse erythroblast cell line. Even though PABPC1 levels and total poly(A) binding protein activity in these MEL cells were essentially unaffected by the PABPC4 depletion (Fig. 2), we identified a significant impact on the steady-state expression of a subset of its mRNA transcriptome (Table 2). Furthermore, analysis of mRNA content in immuno-enriched PABPC4 complexes revealed that a subset of these PABPC4-impacted mRNAs were associated with PABPC4 *in vivo* (Table 2). These data demonstrate that PABPC4 has an essential and nonredundant role in establishing the steady-state transcriptome in a mammalian cell line.

MEL cells have been extensively used to study the process of terminal erythroid maturation (20, 21). The addition of chemical reagents such as DMSO promotes their terminal differentiation. We found that PABPC4 depletion blunts terminal erythroid maturation in MEL cells (Fig. 7A and B) and alters the cellular mRNA transcriptome (Table 2). In particular, we demonstrated that five erythropoiesis-specific genes that are dramatically induced during normal erythroid maturation of MEL cells are each significantly repressed in PABPC4 depleted pools (Fig. 8A to E). Induction of terminal differentiation is dependent on the repression of a well-defined set of genes that support erythroblast replication (48). These genes encode c-Kit, c-Myb, c-Myc, CD44, and Stat5a. The repression of the receptor tyrosine kinase c-Kit and its ligand stem cell factor (SCF) are essential to the linked processes of mitotic arrest and induction of terminal erythroid differentiation (49, 50). c-Kit mRNA was remarkable in that it was abnormally elevated following PABPC4 depletion and remained significantly higher than in the control cell population after DMSO induction. Thus, interference with normal c-Kit repression by PABPC4 depletion is likely to contribute to repressed terminal erythroid maturation and the associated inhibition of key erythroid gene activity.

We next explored the basis for the selective targeting of

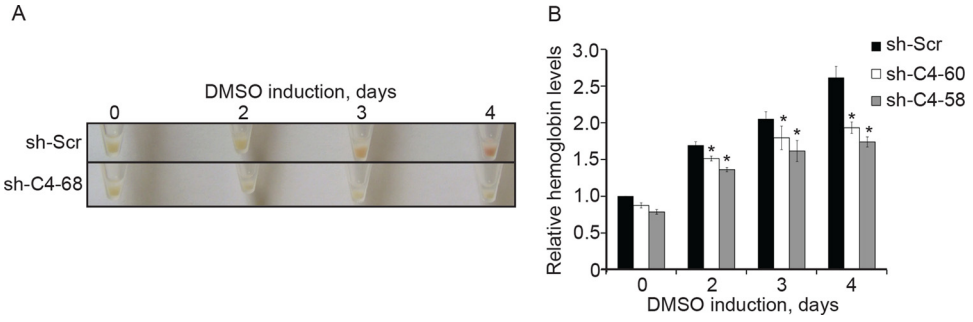

FIG 7 PABPC4 depletion blunts MEL cell differentiation. (A) Visual comparison of cell pellets of PABPC4-depleted MEL cells (sh-C4-68) with cells infected in parallel with virus containing the scrambled control (sh-Scr). (B) Diminished hemoglobin accumulation in PABPC4-depleted DMSO-induced MEL cells pools expressing sh-C4-60 and sh-C4-58, quantified by Drabkin's assay. The *y* axis represents hemoglobin expression relative to sh-Scr at time zero. Asterisks denote *P* values (one tailed *t* test) less than 0.05 for the PABPC4 knockdown pools compared to the sh-Scr cell pools at the corresponding time points. The hemoglobin quantification for the sh-C4-68 pool (data not shown) was consistent with those for the sh-C4-58 and sh-C4-60 pools.

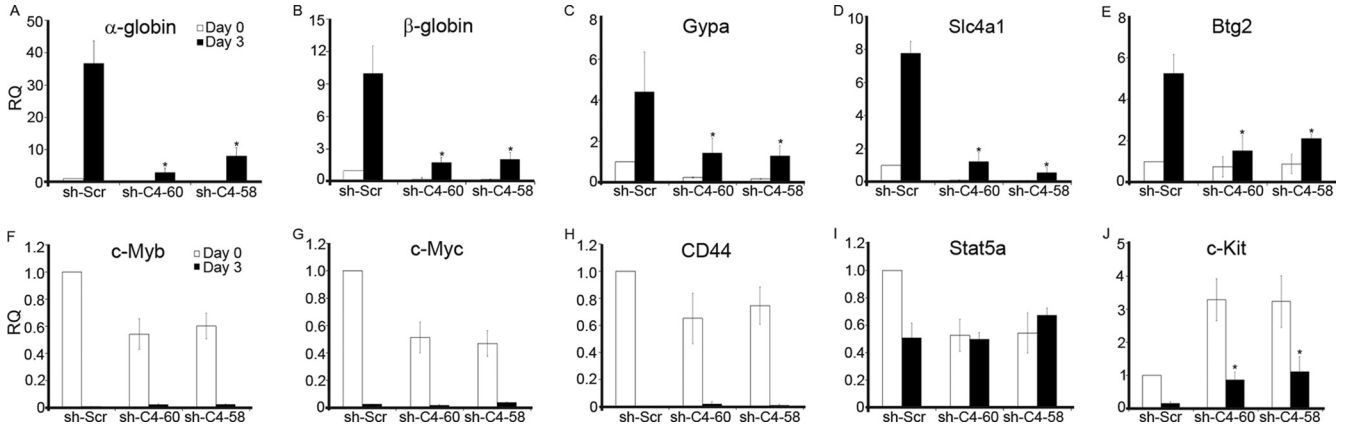

FIG 8 PABC4 depletion in MEL cells impacts the expression of a subset of mRNAs linked to erythroid differentiation. MEL pools expressing control shRNA (sh-Scr) or each of two different PABPC4-targeting shRNAs (sh-C4-60 and sh-C4-58) were assayed after 3 days of DMSO treatment. qRT-PCR analyses were carried out on a group of mRNAs encoding key erythropoiesis-specific proteins that are normally induced during terminal erythroid differentiation (A to E) and a second group of mRNAs that are normally repressed during this developmental window (F to J). The relative quatification (RQ) value for each mRNA (*y* axis) was normalized to its expression in uninduced sh-Scr pools (defined as 1.0). Asterisks denote *P* values (one-tailed *t* test) less than 0.05 for the PABPC4 knockdown pools compared to the corresponding sh-Scr cell pool. Samples were from day 0 (uninduced) and day 3 (DMSO induced).

PABPC4 activities to a subset of mRNAs. Our MEME analysis revealed an AU-rich motif within the 3′ UTRs of the mRNAs that associate with PABPC4 *in vivo* (Fig. 5A). Further analysis revealed that this motif enhances PABPC4 binding to an mRNA with a critically shortened poly(A) tail without a corresponding effect on binding by PABPC1. PABPs interact with the RNAs through their RRMs 1 to 4 (51, 52). RRMs 1 and 2 are highly conserved among the PABP isoforms and confer binding to poly(A) tracts. In contrast, RRMs 3 and 4 are less strictly conserved in structure, and their functions are less well defined. Remarkably, the RRM 3-4 segment of PABPC4 has a higher affinity for AU tracts than the corresponding segment of PABPC1 (K_ds of 2.4 nM versus 3.9 nM) (40). This higher relative affinity of RRMs 3 and 4 of PABPC4 for AU tracts is consistent with the ability of an AU-rich motif to selectively enhance PABPC4 binding to a critically shortened poly(A) tail (Fig. 5C) and to protect mRNAs with critically shortened poly(A) tails from accelerated decay (Fig. 4A to D). This effect of PABPC4 binding on the mutated polyadenylation signal, AAUAAA, while apparent for the *IRF7* 3′ UTR with a critically shortened A_{12} tail (which accentuates the effect of the mutation to the polyadenylation signal [Fig. 5C]), was not detected in the analysis of binding to the *hα-globin* 3′ UTR with a significantly longer A_{33} tail (Fig. 1C). In sum, these observations support a model in which sequences in *cis* to the poly(A) tracts confer specificity of action for the different PABPs to their binding targets.

Our analysis of the poly(A) tail profiles of select PABPC4 target mRNAs supports a model in which PABPC4 can impact an mRNA species by stabilizing the subpopulation of mRNAs with critically shortened poly(A) tails (Fig. 4A to D). This model is consistent with the evidence that loss of the last remaining PABP from a critically shortened poly(A) tail constitutes a rate-limiting event in mRNA clearance from the cell (53). Interestingly, we found that the poly(A) tail of the β-*globin* mRNA, which is not a direct functional target of PABPC4, is not impacted by PABPC4 depletion (Fig. 4I and J), even though its enrichment in PBPC4 complexes is comparable to that of α-*globin* mRNA (Table 3). This difference may reflect the difference in distribution of the long- and short-poly(A)-tailed mRNA populations for the two mRNAs. Compared to α-*globin* mRNA, β-*globin* mRNA has a higher representation of long A tails (Fig. 4A versus I, sh-Scr PAT lanes). This difference would render β-*globin* mRNA less dependent on PABPC4 than α-*globin* mRNA. These results demonstrate that PABPC4 specifically stabilizes short poly(A) tails of its direct binding target mRNAs, while its impact on other mRNAs may be mediated by distinct and possibly less direct pathways. In the case of β-*globin* mRNA, this indirect pathway may reflect a general inhibition of erythroid gene expression by PABPC4 depletion.

The stabilization of short-poly(A)-tailed mRNAs is one possible mechanism through which PABPC4 regulates its mRNA targets. Our current data do not address the mechanisms for the observed upregulation of a distinct subset of mRNAs in cells depleted of PABPC4. We note, however, that in *Drosophila*, PABP stimulates miRNA-mediated silencing of target mRNAs by facilitating miRISC binding (54). Thus, one of the functions of PABPC4 in MEL cells may be mediated via a positive impact on miRNA function; in this case, the depletion of PABPC4 could lead to a decrease in miRNA-mediated mRNA destabilization in a subset of mRNAs. Current explorations of miRNA content in the erythroid lineage can now be utilized to explore this model (54). It is worth noting that prior studies have identified sets of mRNAs that remain stable and efficiently translated despite having short (<20-nt) poly(A) tails under limiting PABP levels (55, 56). Of note, these mRNAs contain AU-rich poly(A)-limiting elements (PLE) within their 3′ UTRs. Our data support a scenario wherein PABPC4 may act as an enabling PLE-interacting protein, mediating the stability and translation of erythroid mRNAs with critically shortened poly(A) tails.

PABPs have long been thought to mediate housekeeping functions of mRNAs in much the same way as histones were once considered to be limited to generic and static packing of DNA. The present study directly challenges this assumption by presenting evidence for specific and dynamic functions of a specific PABP isoform in the process of erythroid differentiation. The identification in this study of structures and mechanisms involved in the specificity and control of PABPC4 actions on the mRNA transcriptome establishes a platform for subsequent analysis of its

functions in additional models of development and cellular differentiation.

ACKNOWLEDGMENTS

We appreciate the generosity of laboratory members in sharing various reagents and suggestions. We acknowledge the input of the University of Pennsylvania Microarray facility for transcriptome profiling.

This work was supported by NIH MERIT HL 65449 and CA72765 award to S.A.L. H.K.K. is the recipient of a research fellowship from the Cooley's Anemia Foundation.

REFERENCES

1. **Blobel G.** 1973. A protein of molecular weight 78,000 bound to the polyadenylate region of eukaryotic messenger RNAs. Proc. Natl. Acad. Sci. U. S. A. **70:**924–928. http://dx.doi.org/10.1073/pnas.70.3.924.
2. **Gorlach M, Burd CG, Dreyfuss G.** 1994. The mRNA poly(A)-binding protein: localization, abundance, and RNA-binding specificity. Exp. Cell Res. **211:**400–407. http://dx.doi.org/10.1006/excr.1994.1104.
3. **Kuhn U, Wahle E.** 2004. Structure and function of poly(A) binding proteins. Biochim. Biophys. Acta **1678:**67–84. http://dx.doi.org/10.1016/j.bbaexp.2004.03.008.
4. **Voeltz GK, Ongkasuwan J, Standart N, Steitz JA.** 2001. A novel embryonic poly(A) binding protein, ePAB, regulates mRNA deadenylation in Xenopus egg extracts. Genes Dev. **15:**774–788. http://dx.doi.org/10.1101/gad.872201.
5. **Seli E, Lalioti MD, Flaherty SM, Sakkas D, Terzi N, Steitz JA.** 2005. An embryonic poly(A)-binding protein (ePAB) is expressed in mouse oocytes and early preimplantation embryos. Proc. Natl. Acad. Sci. U. S. A. **102:**367–372. http://dx.doi.org/10.1073/pnas.0408378102.
6. **Vasudevan S, Seli E, Steitz JA.** 2006. Metazoan oocyte and early embryo development program: a progression through translation regulatory cascades. Genes Dev. **20:**138–146. http://dx.doi.org/10.1101/gad.1398906.
7. **Kleene KC, Mulligan E, Steiger D, Donohue K, Mastrangelo MA.** 1998. The mouse gene encoding the testis-specific isoform of poly(A) binding protein (Pabp2) is an expressed retroposon: intimations that gene expression in spermatogenic cells facilitates the creation of new genes. J. Mol. Evol. **47:**275–281. http://dx.doi.org/10.1007/PL00006385.
8. **Yang H, Duckett CS, Lindsten T.** 1995. iPABP, an inducible poly(A)-binding protein detected in activated human T cells. Mol. Cell. Biol. **15:**6770–6776.
9. **Blanco P, Sargent CA, Boucher CA, Howell G, Ross M, Affara NA.** 2001. A novel poly(A)-binding protein gene (PABPC5) maps to an X-specific subinterval in the Xq21.3/Yp11.2 homology block of the human sex chromosomes. Genomics **74:**1–11. http://dx.doi.org/10.1006/geno.2001.6530.
10. **Wells SE, Hillner PE, Vale RD, Sachs AB.** 1998. Circularization of mRNA by eukaryotic translation initiation factors. Mol. Cell **2:**135–140. http://dx.doi.org/10.1016/S1097-2765(00)80122-7.
11. **Wakiyama M, Imataka H, Sonenberg N.** 2000. Interaction of eIF4G with poly(A)-binding protein stimulates translation and is critical for Xenopus oocyte maturation. Curr. Biol. **10:**1147–1150. http://dx.doi.org/10.1016/S0960-9822(00)00701-6.
12. **Kahvejian A, Svitkin YV, Sukarieh R, M'Boutchou MN, Sonenberg N.** 2005. Mammalian poly(A)-binding protein is a eukaryotic translation initiation factor, which acts via multiple mechanisms. Genes Dev. **19:**104–113. http://dx.doi.org/10.1101/gad.1262905.
13. **Valentini SR, Casolari JM, Oliveira CC, Silver PA, McBride AE.** 2002. Genetic interactions of yeast eukaryotic translation initiation factor 5A (eIF5A) reveal connections to poly(A)-binding protein and protein kinase C signaling. Genetics **160:**393–405. http://www.genetics.org/content/160/2/393.long.
14. **Coller JM, Gray NK, Wickens MP.** 1998. mRNA stabilization by poly(A) binding protein is independent of poly(A) and requires translation. Genes Dev. **12:**3226–3235. http://dx.doi.org/10.1101/gad.12.20.3226.
15. **Kimura M, Ishida K, Kashiwabara S, Baba T.** 2009. Characterization of two cytoplasmic poly(A)-binding proteins, PABPC1 and PABPC2, in mouse spermatogenic cells. Biol. Reprod. **80:**545–554. http://dx.doi.org/10.1095/biolreprod.108.072553.
16. **Gorgoni B, Richardson WA, Burgess HM, Anderson RC, Wilkie GS, Gautier P, Martins JP, Brook M, Sheets MD, Gray NK.** 2011. Poly(A)-binding proteins are functionally distinct and have essential roles during vertebrate development. Proc. Natl. Acad. Sci. U. S. A. **108:**7844–7849. http://dx.doi.org/10.1073/pnas.1017664108.
17. **Passegue E, Wagers AJ.** 2006. Regulating quiescence: new insights into hematopoietic stem cell biology. Dev. Cell **10:**415–417. http://dx.doi.org/10.1016/j.devcel.2006.03.002.
18. **Williamson AJ, Smith DL, Blinco D, Unwin RD, Pearson S, Wilson C, Miller C, Lancashire L, Lacaud G, Kouskoff V, Whetton AD.** 2008. Quantitative proteomics analysis demonstrates post-transcriptional regulation of embryonic stem cell differentiation to hematopoiesis. Mol. Cell. Proteomics **7:**459–472. http://dx.doi.org/10.1074/mcp.M700370-MCP200.
19. **Ostareck-Lederer A, Ostareck DH.** 2004. Control of mRNA translation and stability in haematopoietic cells: the function of hnRNPs K and E1/E2. Biol. Cell **96:**407–411. http://dx.doi.org/10.1016/j.biolcel.2004.03.010.
20. **Friend C, Scher W, Holland JG, Sato T.** 1971. Hemoglobin synthesis in murine virus-induced leukemic cells in vitro: stimulation of erythroid differentiation by dimethyl sulfoxide. Proc. Natl. Acad. Sci. U. S. A. **68:**378–382. http://dx.doi.org/10.1073/pnas.68.2.378.
21. **Marks PA, Rifkind RA.** 1978. Erythroleukemic differentiation. Annu. Rev. Biochem. **47:**419–448. http://dx.doi.org/10.1146/annurev.bi.47.070178.002223.
22. **Marks PA, Rifkind RA.** 1989. Induced differentiation of erythroleukemia cells by hexamethylene bisacetamide: a model for cytodifferentiation of transformed cells. Environ. Health Perspect. **80:**181–188. http://dx.doi.org/10.1289/ehp.8980181.
23. **Kiledjian M, Wang X, Liebhaber SA.** 1995. Identification of two KH domain proteins in the alpha-globin mRNP stability complex. EMBO J. **14:**4357–4364.
24. **Kong J, Ji X, Liebhaber SA.** 2003. The KH-domain protein alpha CP has a direct role in mRNA stabilization independent of its cognate binding site. Mol. Cell. Biol. **23:**1125–1134. http://dx.doi.org/10.1128/MCB.23.4.1125-1134.2003.
25. **Weiss IM, Liebhaber SA.** 1995. Erythroid cell-specific mRNA stability elements in the alpha 2-globin 3′ nontranslated region. Mol. Cell. Biol. **15:**2457–2465.
26. **Ji X, Kong J, Liebhaber SA.** 2003. In vivo association of the stability control protein alphaCP with actively translating mRNAs. Mol. Cell. Biol. **23:**899–907. http://dx.doi.org/10.1128/MCB.23.3.899-907.2003.
27. **Morales J, Russell JE, Liebhaber SA.** 1997. Destabilization of human alpha-globin mRNA by translation anti-termination is controlled during erythroid differentiation and is paralleled by phased shortening of the poly(A) tail. J. Biol. Chem. **272:**6607–6613. http://dx.doi.org/10.1074/jbc.272.10.6607.
28. **Morita S, Kojima T, Kitamura T.** 2000. Plat-E: an efficient and stable system for transient packaging of retroviruses. Gene Ther. **7:**1063–1066. http://dx.doi.org/10.1038/sj.gt.3301206.
29. **Hovhannisyan RH, Carstens RP.** 2007. Heterogeneous ribonucleoprotein m is a splicing regulatory protein that can enhance or silence splicing of alternatively spliced exons. J. Biol. Chem. **282:**36265–36274. http://dx.doi.org/10.1074/jbc.M704188200.
30. **Caputi M, Mayeda A, Krainer AR, Zahler AM.** 1999. hnRNP A/B proteins are required for inhibition of HIV-1 pre-mRNA splicing. EMBO J. **18:**4060–4067. http://dx.doi.org/10.1093/emboj/18.14.4060.
31. **Bolstad BM, Irizarry RA, Astrand M, Speed TP.** 2003. A comparison of normalization methods for high density oligonucleotide array data based on variance and bias. Bioinformatics **19:**185–193. http://dx.doi.org/10.1093/bioinformatics/19.2.185.
32. **Janicke A, Vancuylenberg J, Boag PR, Traven A, Beilharz TH.** 2012. ePAT: a simple method to tag adenylated RNA to measure poly(A)-tail length and other 3′ RACE applications. RNA **18:**1289–1295. http://dx.doi.org/10.1261/rna.031898.111.
33. **Kong J, Liebhaber SA.** 2007. A cell type-restricted mRNA surveillance pathway triggered by ribosome extension into the 3′ untranslated region. Nat. Struct. Mol. Biol. **14:**670–676. http://dx.doi.org/10.1038/nsmb1256.
34. **Katzenellenbogen RA, Vliet-Gregg P, Xu M, Galloway DA.** 2010. Cytoplasmic poly(A) binding proteins regulate telomerase activity and cell growth in human papillomavirus type 16 E6-expressing keratinocytes. J. Virol. **84:**12934–12944. http://dx.doi.org/10.1128/JVI.01377-10.
35. **Xu R, Jin J, Hu W, Sun W, Bielawski J, Szulc Z, Taha T, Obeid LM, Mao C.** 2006. Golgi alkaline ceramidase regulates cell proliferation and survival by controlling levels of sphingosine and S1P. FASEB J. **20:**1813–1825. http://dx.doi.org/10.1096/fj.05-5689com.
36. **Irie J, Reck B, Wu Y, Wicker LS, Howlett S, Rainbow D, Feingold E, Ridgway WM.** 2008. Genome-wide microarray expression analysis of

CD4+ T Cells from nonobese diabetic congenic mice identifies Cd55 (Daf1) and Acadl as candidate genes for type 1 diabetes. J. Immunol. **180:**1071–1079. http://www.jimmunol.org/content/180/2/1071.long.

37. **Chaudhary A, Hilton MB, Seaman S, Haines DC, Stevenson S, Lemotte PK, Tschantz WR, Zhang XM, Saha S, Fleming T, St Croix B.** 2012. TEM8/ANTXR1 blockade inhibits pathological angiogenesis and potentiates tumoricidal responses against multiple cancer types. Cancer Cell **21:** 212–226. http://dx.doi.org/10.1016/j.ccr.2012.01.004.
38. **Liang SY, Moghimi B, Crusselle-Davis VJ, Lin IJ, Rosenberg MH, Li X, Strouboulis J, Huang S, Bungert J.** 2009. Defective erythropoiesis in transgenic mice expressing dominant-negative upstream stimulatory factor. Mol. Cell. Biol. **29:**5900–5910. http://dx.doi.org/10.1128/MCB.00419-09.
39. **Gregory T, Yu C, Ma A, Orkin SH, Blobel GA, Weiss MJ.** 1999. GATA-1 and erythropoietin cooperate to promote erythroid cell survival by regulating bcl-xL expression. Blood **94:**87–96.
40. **Sladic RT, Lagnado CA, Bagley CJ, Goodall GJ.** 2004. Human PABP binds AU-rich RNA via RNA-binding domains 3 and 4. Eur. J. Biochem. **271:**450–457. http://dx.doi.org/10.1046/j.1432-1033.2003.03945.x.
41. **Sachs AB, Davis RW, Kornberg RD.** 1987. A single domain of yeast poly(A)-binding protein is necessary and sufficient for RNA binding and cell viability. Mol. Cell. Biol. **7:**3268–3276.
42. **Mootha VK, Lindgren CM, Eriksson KF, Subramanian A, Sihag S, Lehar J, Puigserver P, Carlsson E, Ridderstrale M, Laurila E, Houstis N, Daly MJ, Patterson N, Mesirov JP, Golub TR, Tamayo P, Spiegelman B, Lander ES, Hirschhorn JN, Altshuler D, Groop LC.** 2003. PGC-1alpha-responsive genes involved in oxidative phosphorylation are coordinately downregulated in human diabetes. Nat. Genet. **34:**267–273. http://dx.doi.org/10.1038/ng1180.
43. **Subramanian A, Tamayo P, Mootha VK, Mukherjee S, Ebert BL, Gillette MA, Paulovich A, Pomeroy SL, Golub TR, Lander ES, Mesirov JP.** 2005. Gene set enrichment analysis: a knowledge-based approach for interpreting genome-wide expression profiles. Proc. Natl. Acad. Sci. U. S. A. **102:**15545–15550. http://dx.doi.org/10.1073/pnas.0506580102.
44. **Ivanova NB, Dimos JT, Schaniel C, Hackney JA, Moore KA, Lemischka IR.** 2002. A stem cell molecular signature. Science **298:**601–604. http://dx.doi.org/10.1126/science.1073823.
45. **Sengupta S, den Boon JA, Chen IH, Newton MA, Dahl DB, Chen M, Cheng YJ, Westra WH, Chen CJ, Hildesheim A, Sugden B, Ahlquist P.** 2006. Genome-wide expression profiling reveals EBV-associated inhibition of MHC class I expression in nasopharyngeal carcinoma. Cancer Res. **66:**7999–8006. http://dx.doi.org/10.1158/0008-5472.CAN-05-4399.
46. **Douglas D, Hsu JH, Hung L, Cooper A, Abdueva D, van Doorninck J, Peng G, Shimada H, Triche TJ, Lawlor ER.** 2008. BMI-1 promotes Ewing sarcoma tumorigenicity independent of CDKN2A repression. Cancer Res. **68:**6507–6515. http://dx.doi.org/10.1158/0008-5472.CAN-07-6152.
47. **Hino M, Nishizawa Y, Tatsumi N, Tojo A, Morii H.** 1995. Down-modulation of c-kit mRNA and protein expression by erythroid differentiation factor/activin A. FEBS Lett. **374:**69–71. http://dx.doi.org/10.1016/0014-5793(95)01078-S.
48. **Hattangadi SM, Wong P, Zhang L, Flygare J, Lodish HF.** 2011. From stem cell to red cell: regulation of erythropoiesis at multiple levels by multiple proteins, RNAs, and chromatin modifications. Blood **118:**6258–6268. http://dx.doi.org/10.1182/blood-2011-07-356006.
49. **Galli SJ, Zsebo KM, Geissler EN.** 1994. The kit ligand, stem cell factor. Adv. Immunol. **55:**1–96.
50. **Munugalavadla V, Dore LC, Tan BL, Hong L, Vishnu M, Weiss MJ, Kapur R.** 2005. Repression of c-kit and its downstream substrates by GATA-1 inhibits cell proliferation during erythroid maturation. Mol. Cell. Biol. **25:**6747–6759. http://dx.doi.org/10.1128/MCB.25.15.6747-6759.2005.
51. **Burd CG, Matunis EL, Dreyfuss G.** 1991. The multiple RNA-binding domains of the mRNA poly(A)-binding protein have different RNA-binding activities. Mol. Cell. Biol. **11:**3419–3424.
52. **Nietfeld W, Mentzel H, Pieler T.** 1990. The Xenopus laevis poly(A) binding protein is composed of multiple functionally independent RNA binding domains. EMBO J. **9:**3699–3705.
53. **Decker CJ, Parker R.** 1993. A turnover pathway for both stable and unstable mRNAs in yeast: evidence for a requirement for deadenylation. Genes Dev. **7:**1632–1643. http://dx.doi.org/10.1101/gad.7.8.1632.
54. **Moretti F, Kaiser C, Zdanowicz-Specht A, Hentze MW.** 2012. PABP and the poly(A) tail augment microRNA repression by facilitated miRISC binding. Nat. Struct. Mol. Biol. **19:**603–608. http://dx.doi.org/10.1038/nsmb.2309.
55. **Peng J, Schoenberg DR.** 2005. mRNA with a <20-nt poly(A) tail imparted by the poly(A)-limiting element is translated as efficiently in vivo as long poly(A) mRNA. RNA **11:**1131–1140. http://dx.doi.org/10.1261/rna.2470905.
56. **Gupta JD, Gu H, Schoenberg DR.** 2001. Position and sequence requirements for poly(A) length regulation by the poly(A) limiting element. RNA **7:**1034–1042. http://dx.doi.org/10.1017/S1355838201010329.